Proton-lattice relaxation in NH_4MF_3

1989 J. Phys.: Condens. Matter 1 1119

(http://iopscience.iop.org/0953-8984/1/6/010)

J. Phys.: Condens. Matter **1** (1989) 1119–1132. Printed in the UK

Proton–lattice relaxation in NH_4MF_3

Elías Palacios†, Juan Bartolomé†, Ramón Burriel† and Hans B Brom‡

† Instituto de Ciencia de Materiales de Aragón (ICMA), ETSIIZ-Facultad de Ciencias, Universidad de Zaragoza-CSIC, María Zambrano 50, 50015-Zaragoza, Spain

‡ Kamerlingh Onnes Laboratorium, Niewsteeg 18, Leiden, The Netherlands

Received 13 July 1988

Abstract. Nuclear magnetic resonance measurements of the proton–lattice relaxation times T_1 and $T_{1\rho}$ in NH_4MgF_3 and NH_4ZnF_3 between 40 and 150 K and in NH_4CdF_3 between 70 and 300 K are presented. The relaxation was found to be non-exponential, but fitted very well to a sum of two exponentials. Data were analysed in a three-bath model. Activation energies E_a of 760 ± 50 K, 825 ± 20 K and 1950 ± 50 K in their low-temperature phases were found for the three compounds, respectively. The trend to an increase of E_a with increasing unit-cell size is in contradiction with the expected trend from calculations using atom–atom electrostatic potentials. The average tunnel frequencies are consistent with activation energies. Short-range forces acting between H^+ and F^- are assumed in order to explain these results.

1. Introduction

A great amount of work has been devoted to the family of cubic perovskites NH_4MF_3 (M = divalent cation) since they offer a good opportunity of verifying experimentally the quantum-mechanical dynamics of a rotor in a highly symmetric three-dimensional potential.

The compounds with M = Mg, Zn, Co, Mn and Cd have a cubic high-temperature phase (space group Pm3m, figure 1) and upon cooling undergo a structural first-order transition to a lower symmetry. The structural parameters and transition temperatures T_c were determined from heat capacity C_p measurements (Bartolomé *et al* 1977, 1983, Navarro *et al* 1986, Palacios *et al* 1986), and neutron diffraction (ND) and x-ray diffraction (XRD) measurements (Helmholdt *et al* 1980). They are listed in table 1 for the relevant cases in the present paper.

The trend of increasing critical temperatures for increasing cell dimensions observed has been used to argue that the structural transition is caused mainly by ion-packing instabilities following the Goldschmidt parameter criteria (Helmholdt *et al* 1980) rather than caused by NH_4^+–NH_4^+ coupling, as found in ammonium halides.

The low-temperature phase symmetry is distorted with respect to the cubic phase through small tilts of the MF_6 octahedra, in a similar way to other related trifluorides such as NH_4MnCl_3 (Tornero *et al* 1978) or $KMnF_3$ (Hidaka *et al* 1986). The structural group P4*bm* has been tentatively proposed after single-crystal x-ray diffraction measurements (Tornero and Fayos 1988). This symmetry is consistent with the presence of weak

0953-8984/89/061119 + 14 $02.50

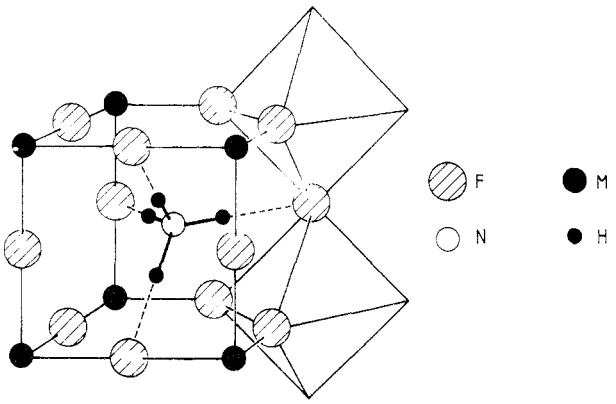

Figure 1. Scheme of the structure of the high-temperature phase of NH_4MF_3 with M = Mg, Zn, Cd. Some MF_6 octahedra are drawn. Broken lines show the shortest H^+–F^- distances.

Table 1. Cell parameters, transition temperatures, activation energies (from relaxation times) and tunnelling frequencies of several NH_4MF_3 compounds. The main experimental results of the present work are in **bold**.

	NH_4MgF_3	NH_4ZnF_3	NH_4CdF_3
Cubic			
a (Å)	4.056[a]	4.118[b]	**4.390 ± 0.002**
T_c (K)	107.5[a]	115.1[c]	331.2[a]
E_a (K)	**450 ± 50**	680 ± 20[d]	
		650[e]	
		580[f]	
E_a (K)$_{BNB}$	583	490	295
τ_0 (s)		4×10^{-14} [d]	
		7×10^{-14} [e]	
		5.2×10^{-14} [f]	
Distorted			
a (Å)	4.026[a]	4.0808[b]	**4.368 ± 0.001**
c (Å)	4.080[a]	4.150[b]	**4.430 ± 0.001**
E_a (K)	850[g]	825 ± 35[d]	
	760 ± 50	**825 ± 20**	**1950 ± 50**
E_a (K)$_{BNB}$	649	650	369
τ_0 (s)		4×10^{-14} [d]	
		7×10^{-14} [e]	
	2×10^{-13}	**1×10^{-13}**	**2.4×10^{-14}**
E_1 (K)	**150 ± 70**	**200 ± 70**	**1100 ± 1100**
ω_t (s^{-1})	**$(1.1 \pm 0.1) \times 10^7$**	**$(8.5 \pm 0.1) \times 10^6$**	**$\sim 5 \times 10^5$**
ω_1 (s^{-1})	1.07×10^5 [h]	1.07×10^5 [h]	2.33×10^5 [i]
D_{inter} (s^{-1})		3000	3000

[a] Palacios *et al* (1986).
[b] Helmholdt *et al* (1980).
[c] Bartolomé *et al* (1977).
[d] NMR: Brom and Bartolomé (1981).
[e] NMR: Raaen *et al* (1982).
[f] QNS: Steenbergen *et al* (1979).
[g] Palacios *et al* (1984).
[h] Measurements with $B_1 = 4 \times 10^{-4}$ T.
[i] Measurements with $B_1 = 8.7 \times 10^{-4}$ T.

ferromagnetism (Bartolomé *et al* 1983) as well as with the data analysis of the low-temperature Raman spectra of the internal NH_4^+ vibrations, where its site symmetry is found to be C_s (Knop *et al* 1981, Agulló-Rueda *et al* 1988).

The C_p data analysis showed a contribution caused by the hindered rotation of the NH_4^+ ions above T_c. Besides, an unusually high latent heat with anomalous molar entropy $\Delta S/R \simeq \ln 3 = 1.10$ (R = gas constant) was observed for all members of the family while, in contrast, typical values of $\Delta S/R = 0.1$ are reported for non-ammonium perovskites. The excess value is attributed to the reorientation of NH_4^+ groups which in the distorted phase have a lower number of minimum-energy orientations than in the cubic one.

This interpretation was corroborated with quasi-elastic neutron scattering (QNS) experiments (Steenbergen *et al* 1979) performed on NH_4ZnF_3. The activation energy of the stochastic jumps across the hindering barrier and the residence time were derived for the high-temperature phase ($E_0 = 580$ K; $\tau_0 = 5.2 \times 10^{-14}$ s).

By means of proton–lattice relaxation measurements with the pulsed nuclear magnetic resonance (NMR) technique (Brom and Bartolomé 1981), a somewhat higher activation energy was deduced ($E_a = 680 \pm 20$ K) for the high-temperature phase and $E_a = 825 \pm 35$ K for the low-temperature phase. Both determinations were later corroborated (Raaen *et al* 1982) though their values were slightly lower (see table 1). Finally, the same type of measurements were performed on polycrystalline NH_4MgF_3, yielding $E_a = 850$ K below T_c (Palacios *et al* 1984).

To explain all these experimental results a simplified model was proposed by Bartolomé, Navarro and Burriel (BNB model) (Bartolomé *et al* 1977, Burriel *et al* 1984) in which each NH_4^+ behaved like a quantum spherical top under the hindering potential produced by the electrostatic interaction between protons and the other lattice ions which were considered as fixed point charges. It gave a satisfactory account of the high-temperature NH_4^+ dynamical behaviour. Also the trend of increasing barriers for decreasing cell size, deduced from NMR, indicated the adequacy of the model, although the difference in the E_a values was probably within the experimental error bars as we know today.

On the other hand, the predicted anomalous entropy content $\Delta S/R \simeq \ln \frac{3}{2}$ was much lower than the measured one. This was caused by the earlier simplification (Bartolomé *et al* 1977) of the low-temperature structure to a simple tetragonal elongation which yielded four equivalent distinguishable orientations while the low-temperature symmetry is known to be orthorhombic. A recent paper (Navarro *et al* 1987) discusses in detail the weak points of the BNB model as far as the C_p results are concerned.

Other noteworthy contradictions are found in the Raman experiments performed on NH_4ZnF_3 and NH_4MnF_3 single crystals at room temperature (Bartolomé *et al* 1985) and under high pressure ($P_{max} \simeq 20$ GPa) (Palacios *et al* 1987). One finds that the NH_4^+ internal stretching vibration frequencies (ν_1, ν_3) *decrease* with increasing unit-cell size (i.e. with increasing N–F distance), while in the electrostatic model the opposite trend is predicted since the reduction of the H . . . F force should encompass the strengthening of the N–H bond. All these facts suggest that the point-charge model has to be thoroughly revised.

The faltering of the BNB model needs a clear-cut example to determine its limitations. For this purpose the compound NH_4CdF_3 is ideal since it has the largest unit cell and highest T_c of the series. Moreover, being non-magnetic, it is a good candidate for pulsed NMR studies of the proton motion.

Given the improvements of the experimental equipment with respect to the previous

measurements on the Zn and Mg compounds, it was deemed convenient to remeasure both and compare the fresh results to the Cd ones obtained under the same conditions.

2. Experimental details

The NH_4MgF_3 sample was obtained by heating a powdered homogeneous mixture of NH_4HF_2 and MgF_2 at 420 K (Rudorff *et al* 1963). The NH_4CdF_3 sample was prepared by heating a mixture of CdF_2 and NH_4F up to 420 K (Cousseins and Piña-Pérez 1968). The excess of NH_4F was removed by washing with methanol and heating the sample at 400 K for several hours. The NH_4ZnF_3 was obtained from a solution of fresh $ZnBr_2$ and NH_4F in methanol.

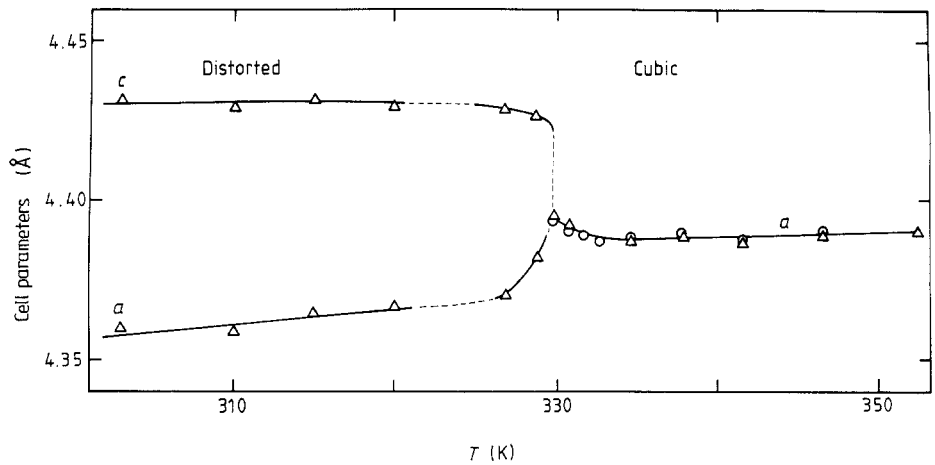

Figure 2. Variation of the cell parameters of NH_4CdF_3 with temperature in the neighbourhood of the transition. Different symbols for two runs are used in the high-temperature phase.

From the C_p measurements of NH_4CdF_3 the observation of the lambda anomaly allowed one to conjecture that this compound had a transition from a pseudo-tetragonal structure (Cousseins and Piña-Pérez 1968) to the high-temperature cubic phase, which had not been measured so far. Then, x-ray powder diffraction data were taken at temperatures below and above T_c (figure 2) (Fruchart 1988). The values at 317 and 333 K are given in table 1. The elongation of the unit cell in the low-temperature phase ($c/a = 1.104$) is similar to the elongation found on the other series members.

3. Proton–lattice relaxation: experimental results

3.1. NH_4MgF_3

The Zeeman proton relaxation time in the laboratory frame, T_1, was measured using a spin–echo pulse spectrometer at a frequency of $\omega_0/2\pi = 10$ MHz with a π—τ—$\pi/2$ sequence. The relaxation time in the rotating frame, $T_{1\rho}$, was measured with a $\pi/2$ spin-

lock pulse sequence and a RF field amplitude $B_1 = 4 \times 10^{-4}$ T. Some data with $B_1 = 8 \times 10^{-4}$ and 12×10^{-4} T were also taken in order to establish the dependence of $T_{1\rho}$ on ω_1 ($=\gamma B_1$, γ = proton gyromagnetic ratio, B_1 = amplitude of the RF field). The temperature range scanned was between 4 and 150 K. The results are depicted in figure 3 in the conventional $\log(T_1)$ versus $1/T(\mathrm{K}^{-1})$ form. The main features are as follows.

(i) The phase transition is seen as a change in slope in the $\log(T_1)$ versus $1/T$ curve. Above T_c the linear behaviour observed may be fitted with the classical expression for the intra-ammonium proton relaxation (BPP model, from Bloemberger, Purcell and Pound) (O'Reilly and Tsang 1967) on its high-temperature limit:

$$\frac{1}{T_1} = A\left(\frac{\tau}{1+\omega_0^2\tau^2} + \frac{4\tau}{1+4\omega_0^2\tau^2}\right) \tag{1}$$

$$\frac{1}{T_{1\rho}} = A\left(\frac{5}{2}\frac{\tau}{1+\omega_0^2\tau^2} + \frac{\tau}{1+4\omega_0^2\tau^2} + \frac{3}{2}\frac{\tau}{1+4\omega_1^2\tau^2}\right) \tag{2}$$

$$A = (\mu_0/4\pi)^2\, 9\gamma^4\hbar^2/10r^6 \tag{3}$$

where $\gamma = 2.6752 \times 10^8$ rad s^{-1} T^{-1}, $\mu_0/4\pi = 10^{-7}$ T mA^{-1}, r = H–H distance, and $\tau = \tau_0 \exp(E_a/kT)$. The activation energy $E_a = 450 \pm 50$ K was deduced, which is somewhat lower than the one previously determined for NH_4ZnF_3.

It was not possible to determine τ_0 accurately by extrapolation of $\log(T_1)$ to infinite temperature, because the points deviate from theoretical behaviour above 150 K (where $T_1 \simeq 1$ s); however, the order of magnitude ($\tau_0 \simeq 10^{-14}$ s) is derived.

(ii) Below T_c the plot of $\log(T_1)$ against $1/T$ shows a typical minimum and two branches. Between 70 and 107 K (the 'classical region' of T_1) it is not easy to obtain an activation energy because the slope changes continuously close to the structural transition. From the fit to expression (1) one gets the best estimate as curve A in figure 3 with a value $E_a = 760 \pm 50$ K and $\tau_0 \simeq 2 \times 10^{-13}$ s. The value of E_a seems to be lower than previously measured, but it is not sufficiently resolved to decide whether E_a is larger or smaller than in the Zn compound.

(iii) The minimum of T_1 has a value $(T_1)_{\min} = 2.5$ ms which corresponds to $A = 1.76 \times 10^{10}$ s^{-2} and the N–H distance $d(\mathrm{NH}) = \sqrt{(3/8)}r = 1.07$ Å, which is higher than the values usually derived between 1.04 and 1.06 Å. The departure from the classical behaviour is an indication that tunnelling between minima is becoming already significant, as will be discussed below.

(iv) Between 60 and 45 K the relaxation was found to be non-exponential but fitted well to a double exponential with equal pre-exponential factors:

$$M(t) = M_0\{\exp[-t/T_1(\mathrm{l})] + \exp[-t/T_1(\mathrm{sh})]\}.$$

The longer time constant $T_1(\mathrm{l})$ approached the classical behaviour whereas the shorter one $T_1(\mathrm{sh})$ yields a slope of $E_a \simeq 150 \pm 70$ K. This second time constant is difficult to establish accurately when $T_1(\mathrm{sh})$ and $T_1(\mathrm{l})$ have the same order of magnitude. Below 45 K, $\log[T_1(\mathrm{l})]$ also deviates from the classical curve, reaching a smaller slope.

(v) While $T_{1\rho}$ coalesced with T_1 in the high-temperature region, it did not show the classical minimum predicted by the BPP model at $\omega_1\tau \simeq 0.5$ deduced from (2). Indeed, $T_{1\rho}$ showed a 'Haupt's' minimum, independent of ω_1, at $1/T = 18 \times 10^{-3}$ K^{-1}, with a value of $(T_{1\rho})_{\min} = 6 \times 10^{-4}$ s. Shorter relaxation times were barely established because of their small amplitude and because relaxation times shorter than 10^{-4} s are beyond the experimental limit.

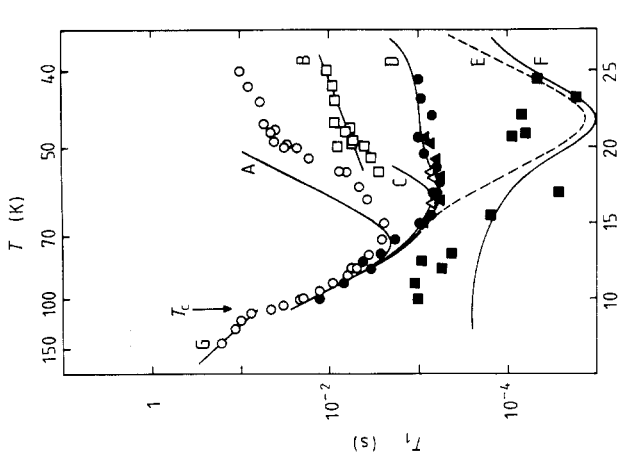

Figure 3. Relaxation times for NH_4MgF_3: ○, T_1(l); □, T_1(sh); ●, $T_{1\rho}$(l) ($B_1 = 4 \times 10^{-4}$ T); △, $T_{1\rho}$(l) ($B_1 = 8 \times 10^{-4}$ T); ▲, $T_{1\rho}$(l) ($B_1 = 12 \times 10^{-4}$ T); ■, $T_{1\rho}$(sh) ($B_1 = 4 \times 10^{-4}$ T). The arrow indicates the transition temperature. Parameters from table 1. The different curves are: A, T_1 from classical BPP prediction (1); B, slope of T_1(sh) (in logarithmic scale) versus $1/T$; C, $T_{1\rho}$(l) from the three-bath model (5), (6) and (7) with $D_{inter} = 0$; D, $T_{1\rho}$(l) from the three-bath model with $D_{inter} = 3000$; E, $T_{1\rho}$ from classical BPP prediction (2); F, $T_{1\rho}$(sh) from the three-bath model with $D_{inter} = 3000$; G, slope of $\log(T_{1\rho})$ in cubic phase.

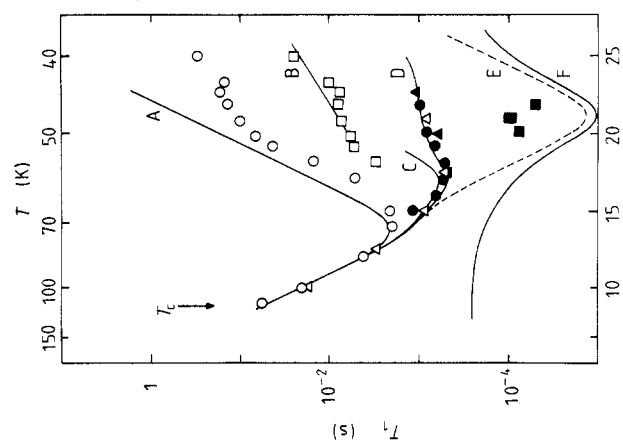

Figure 4. Relaxation times for NH_4ZnF_3: ○, T_1(l); □, T_1(sh); ●, $T_{1\rho}$(l) ($B_1 = 4 \times 10^{-4}$ T); △, $T_{1\rho}$(l) ($B_1 = 25 \times 10^{-4}$ T); ▲, $T_{1\rho}$(l) ($B_1 = 12 \times 10^{-4}$ T); ■, $T_{1\rho}$(sh) ($B_1 = 4 \times 10^{-4}$). The arrow indicates the transition temperature. The different curves are: A, T_1 from classical BPP prediction (1); B, slope of T_1(sh) (in logarithmic scale) versus $1/T$; C, $T_{1\rho}$(l) from the three-bath model (5), (6) and (7) with $D_{inter} = 0$; D, $T_{1\rho}$(l) from the three-bath model with $D_{inter} = 3000$; E, $T_{1\rho}$ from classical BPP prediction (2); F, $T_{1\rho}$(sh) from the three-bath model with $D_{inter} = 3000$.

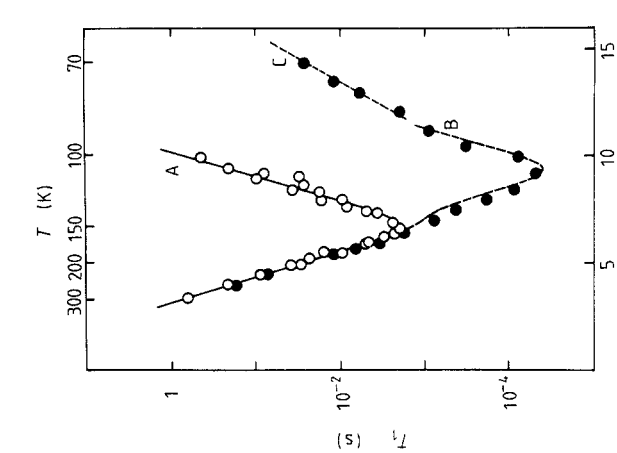

Figure 5. Relaxation times for NH_4CdF_3: ○, T_1; ●, $T_{1\rho}$ ($B_1 = 8.7 \times 10^{-4}$ T). The different curves are: A, T_1 from classical BPP prediction (1); B, $T_{1\rho}$ from Haupt's theory with $\omega_t = 5 \times 10^5$ s^{-1}; C, slope of $\log(T_{1\rho})$ versus $1/T$.

3.2. NH_4ZnF_3

This compound showed similar features to NH_4MgF_3 (see figure 4) though there are some differences:

(i) The experiments were performed below T_c, and thus no new activation energy for the cubic phase could be derived.

(ii) Between 115 and 70 K the $\log(T_1)$ curve approaches the BPP model much better than in the Mg compound, yielding $E_a = 825 \pm 20$ K, in full agreement with our previous determinations, and $\tau_0 \simeq 10^{-13}$ s, like in NH_4MgF_3.

(iii) Like in the Mg compound, between 70 and 45 K the Zeeman relaxation fits well to a double exponential with equal weights at low temperature, showing a longer time constant with quasi-classical dependence on $1/T$ and a shorter one which gives a slope of about $E_1 \simeq 200 \pm 70$ K. Below 45 K, T_1(l) shows the same departure from the BPP model as in the Mg compound.

(iv) $T_{1\rho}$ shows a Haupt's minimum at $1/T = 17.6 \times 10^{-3}\,K^{-1}$ with $(T_{1\rho})_{min} = 5 \times 10^{-4}$ s, which gives a lower tunnel frequency than for NH_4MgF_3 (see discussion).

3.3. NH_4CdF_3

In this compound T_1 and $T_{1\rho}$ showed a quasi-classical behaviour (figure 5):

(i) The activation energy was 1950 ± 50 K, as obtained from the slope of T_1 against $1/T$ well above and well below the minimum.

(ii) The value at the minimum is $(T_1)_{min} = 2$ ms. Using the BPP prediction (1),

$$(T_1)_{min} = 0.7017\omega_0/A \tag{4}$$

yields $A = 2.2 \times 10^{10}\,s^{-2}$ which substituted in (3) gives $d(NH) = 1.04 \pm 0.01$ Å, in good agreement with the commonly accepted value $d(NH) = 1.042$ Å (Garland *et al* 1979). This value is slightly lower than those used by Svare (1977) in $(NH_4)_2MCl_6$, $d(NH) = 1.059$ Å, which gives $A = 1.91 \times 10^{10}\,s^{-2}$.

(iii) The extrapolation of $\log(T_1)$ to $T \to \infty$ gives a correlation constant $\tau_0 \simeq 2.4 \times 10^{-14}$ s, similar to the value obtained in other compounds of very high barriers (Svare 1977).

(iv) $T_{1\rho}$ shows a quasi-classical minimum which agrees fairly well with the BPP prediction (2), taking into account that relaxation times shorter than 10^{-4} s are difficult to measure accurately. Nevertheless $T_{1\rho}$ does not reach the classical minimum value, which allows us to make an estimation for the average tunnel frequency $\omega_t \simeq 5 \times 10^5\,s^{-1}$. The parameters are given in table 1.

From the present result it is clear that NH_4CdF_3 behaves differently than the Zn and Mg compounds, since its relaxation corresponds to high-barrier-hindered motion. Thus one finds the highest barrier for the largest cell in contrast to the BNB model for which it should be lowest. This is the main result of the present experiment.

(v) Below 90 K the slope of $\log T_{1\rho}$ gives an activation energy of about 1100 ± 100 K, probably due to tunnelling between torsional excited states, which modifies the correlation time.

4. Analysis

In the previous section a systematic comparison with the BPP model shows up the

deviations in the three compounds due to quantum effects. Here they are analysed in terms of existing models.

The simplest model that considers quantum tunnelling of molecular groups was developed by Haupt (1971), under the assumption that a common spin temperature may be reached. The model was also used to compute T_1 in ammonium ions (Punkkinen 1975). It is demonstrated that the correlation time for tunnel reorientations through the first excited torsional state is given by the rate of phonon-induced transitions between the zeroth and first excited levels. Thus, classical jumps are very unlikely at low temperatures and the energy difference between these levels (E_1) would be observed as an 'activation energy'.

For the NH_4^+ ion the four-proton spin species can be classified with respect to a point group of T symmetry (subgroup of T_d since a rigid ion is considered). One has five singlets A (total spin $I = 2$), three triplets T ($I = 1$) and a doublet E (two states with $I = 0$) (Press 1982). The assumption of a common spin temperature between the species implies the existence of very effective inter-NH_4^+ cross-relaxation processes which would lead to the observation of just one time constant T_1. This condition is apparently fulfilled for all the compounds above the temperature of the BPP minimum. The transition rates induced by intra-ammonium dipole–dipole interactions have to be of similar order of magnitude within T species and between A and T states. However, below that temperature the magnetisation decay needs to be described with two exponentials. Riehl *et al* (1973) interpreted this behaviour in terms of a three-bath model, in which different relaxation terms for different spin species are considered. Since the E species has no moment, each exponent is related to one of the A or T species, in the absence of any coupling between them. Actually, the intensity ratio at $t = 0$, $M_s(0)/M_l(0)$, of the two components after the RF pulse may have values ranging from zero for very fast cross relaxation to 1.67 for independent species. Ratios close to 1 for NH_4MgF_3 and NH_4ZnF_3 imply that they are in an intermediate case. The A states do not relax by intra-ammonium dipolar interaction to A states, but to E or T states. When the T $\leftrightarrow$ T relaxation is faster than A $\leftrightarrow$ E or A $\leftrightarrow$ T (probably due to different correlation times), a sum of two exponentials is obtained (Punkkinen 1975).

The rotational potential is perturbed by phonons because they modify slightly the relative positions of the atoms in the cage surrounding the NH_4^+. The rotor–lattice interaction does not act on the nuclear spins, and thus it cannot change the type of symmetry of the rotational wavefunction. One can assume that only acoustic phonons with long wavelengths have frequencies comparable to the librational frequency. They can only excite the T states to the first excited torsional level, because these phonons transform like the irreducible representation T of the symmetry group of NH_4^+, and the direct products T $\times$ A and T $\times$ E do not contain A or E, respectively.

This fact explains why the longer relaxation time approaches the classical BPP curve. It is associated with the relaxation of A spins. The shorter time constant is due to T spins, and the slope of $\log[T_1(\mathrm{sh})]$ versus $1/T$ would equal E_1. The long-time-constant component deviates as well from the BPP behaviour, probably due to coupling between A and T spin species. Though this derivation is somewhat speculative (in addition to experimental errors and coupling between both species, other excited levels should be considered in low-symmetry phases), it is the first estimation of the torsional levels since so far we have not been able to detect them from optical spectroscopy (Bartolomé *et al* 1985) or inelastic neutron scattering. An independent verification of the E_1 values listed in table 1 should then be performed.

The effect of tunnelling in the ground torsional level is to substitute ω_0^2 and $(2\omega_0)^2$

by $(\omega_t \pm \omega_0)^2$ or $(\omega_t \pm 2\omega_0)^2$ in some transition rates, which produces an increase in the value of $(T_1)_{min}$. In NH_4MgF_3, and NH_4ZnF_3 a small increase of $(T_1)_{min}$ over the classical minimum is observed, and none in NH_4CdF_3. However, this is the reason, mentioned above, why the experimental data do not fit the classical curve close to the minimum for NH_4MgF_3.

On the contrary, if $\omega_t \gg \omega_1$ a Haupt's minimum is caused by the substitution of $(2\omega_1)^2$ by $(\omega_t \pm 2\omega_1)^2$ in (2). The non-exponential relaxation of T_1 suggested that the common spin temperature assumption is not correct for NH_4MgF_3 and NH_4ZnF_3. So, the $T_{1\rho}$ data have been analysed under the semi-classical three-bath model (Morimoto 1982), which assumes different relaxation rates for A and T species with coupling k_1 and k_2 with the phonon bath respectively, and k_3 and k_4 with each other. The ratio $k_4/k_3 = I(I+1)_T/I(I+1)_A = 3$ is fixed by the ratio of T and A spins heat capacity. Two different relaxation times are predicted, given by

$$\begin{aligned} 1/T_{1\rho}(\text{sh}) &= \tfrac{1}{2}[B + (B^2 - 4C)^{1/2}] \\ 1/T_{1\rho}(\text{l}) &= \tfrac{1}{2}[B - (B^2 - 4C)^{1/2}] \end{aligned} \tag{5}$$

where $B = k_1 + k_2 + k_3 + k_4$, $C = k_1k_2 + k_2k_3 + k_1k_4$ and

$$\begin{aligned} k_1 &= A\left(\frac{5}{2}\frac{\tau}{1+\omega_0^2\tau^2} + \frac{\tau}{1+4\omega_0^2\tau^2} + \frac{33}{32}\frac{\tau}{1+\omega_t^2\tau^2}\right) \\ k_2 &= k_1 + \tfrac{15}{8}A\tau/(1+4\omega_1^2\tau^2) \\ k_4 &= \tfrac{33}{32}A\tau/(1+\omega_t^2\tau^2) + D_{\text{inter}} \\ k_3 &= \tfrac{1}{3}k_4 \end{aligned} \tag{6}$$

with

$$D_{\text{inter}} = a(\mu_0/4\pi)^2\gamma^4\hbar^2/r_{\text{inter}}^6. \tag{7}$$

In these expressions the parameter ω_t should be taken as an average tunnel frequency. The approximation used (Morimoto 1982) assumes that only transitions between A states and E and T states are important. They are given a common energy ($\Delta_{AE} = \Delta_{Ai} = \hbar\omega_t$, $\Delta_{ij} = 0$, i and j stand for the three different T species).

The parameter D_{inter} is a phenomenological term of spin diffusion caused by the inter-molecular dipolar interactions, which in turn is proportional to the local dipolar field.

For NH_4ZnF_3 and NH_4MgF_3, if one neglects the inter-ammonium coupling ($D_{\text{inter}} = 0$), as $\omega_1 \ll \omega_t \ll \omega_0$ the relaxation is almost exponential at high temperatures because the amplitude of the fast-relaxed signal is very small (see figure 4 in Morimoto 1982).

At low temperature, when $\omega_t\tau \simeq 1$, $\tau/(1+4\omega_1^2\tau^2) \gg \tau/(1+\omega_t^2\tau^2)$ and $k_2 \gg k_1, k_3, k_4$. Hence, upon cooling, $T_{1\rho}$(l) shows the ω_1-independent minimum while $T_{1\rho}$(sh) reaches the classical minimum and then $\log[T_{1\rho}(\text{sh})]$ should increase with a constant slope equal to E_a (curves C in figures 3 and 4). This tendency is not followed by the experimental data, deviating markedly at temperatures below the minimum. However, if one includes a non-zero inter-molecular dipolar interaction a good fit is achieved with $D_{\text{inter}} = 3000\ \text{s}^{-1}$ (curves D in figures 3 and 4). Final fitting parameters are listed in table 1, where ω_t was deduced from the minimum of $T_{1\rho}$(l).

For NH_4CdF_3 this effect is not observed because of the much higher E_a value. Consequently the minimum appears at higher temperature. Then ω_t is very small, so deviations from classical BPP theory are noticeable only in the neighbourhood of $(T_{1\rho})_{min}$. The value $\omega_t \simeq 5 \times 10^5$ is obtained by comparison with the BPP prediction for $(T_{1\rho})_{min}$.

For the Mg and Zn compounds, the ω_t values lie slightly above the empirical formula proposed by Svare (1977)

$$\omega_t = 26.4 \times 10^{12} \exp(-0.464 E_a^{1/2}) \tag{8}$$

with ω_t (s^{-1}) and E_a (K) as shown in figure 6. In ammonium hexachlorides ω_t usually lies above the empirical rule (8) due to the narrow barriers. This seems to be the case for NH_4MgF_3 and NH_4ZnF_3 although the effect is not so clear. The result is consistent with a lower hindering barrier for the Mg compound than for the Zn one, pointing again to a trend of decreasing barrier for decreasing unit-cell size. In NH_4CdF_3 ω_t lies far from the prediction (8), but the experimental value is not very reliable and furthermore the rule (8) probably does not apply in that kind of high-barrier compound.

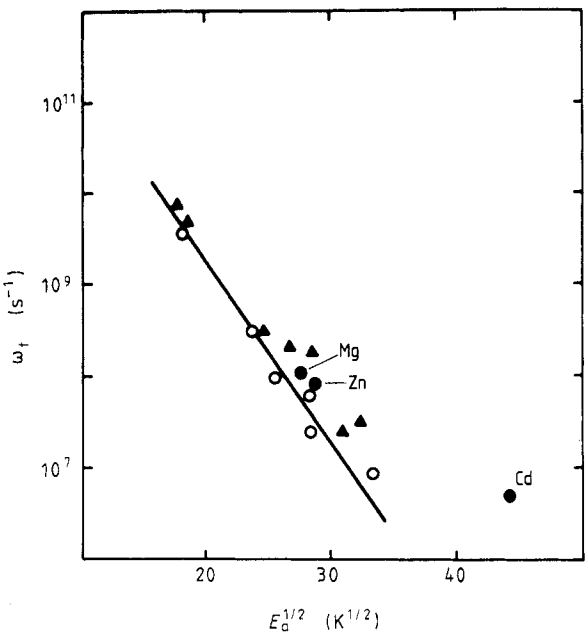

Figure 6. Plot of ω_t (s^{-1}) (logarithmic scale) versus $E_a^{1/2}$ ($K^{1/2}$): ○, several ammonium compounds (Svare 1977); ●, NH_4MF_3 (M = Mg, Zn, Cd); ▲, $(NH_4)_2MCl_6$ (Svare 1977). The straight line represents expression (8).

For ammonium compounds a relation has been proposed between the activation energy and the first excited torsional level which would depend upon the jump geometry (Svare *et al* 1979, Otnes and Svare 1979) (figure 7, line A):

$$E_a = 4.2 \times 10^{-3} E_1^{2.1} \text{ (energies in kelvin).} \tag{9}$$

The activation energies of NH_4MgF_3 and NH_4ZnF_3 (figure 7) fall close to the line B

$$E_a = 1.4\, E_1^{1.22} \tag{10}$$

found for the compounds $(NH_4)_2MCl_6$ and $(NH_4)_2SiF_6$, which are characteristic in presenting narrow barriers between very broad wells (Müller and Hüller 1982).

In $(NH_4)_2MCl_6$ the bottom of the well is broad because there are three Cl^- ions attracting each proton and the potential does not vary much inside the triangle formed

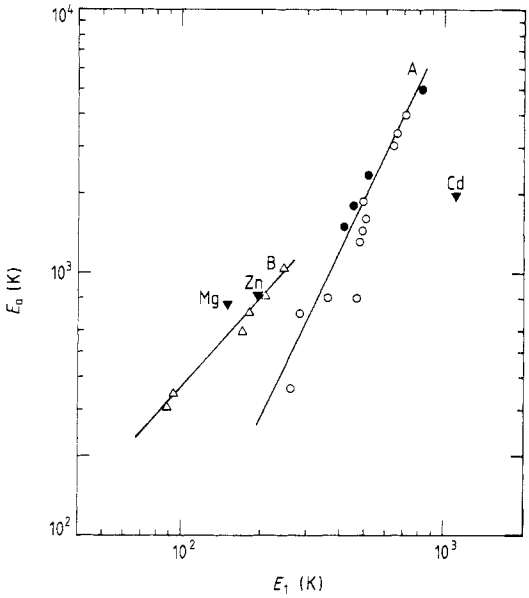

Figure 7. Double logarithmic plot of E_a versus E_1: ●, NH_4X (X = F, Cl, Br, I); △, $(NH_4)_2MCl_6$ (Otnes and Svare 1979); ▼, NH_4MF_3 (M = Mg, Zn, Cd); ○, other ammonium compounds (Svare 1979). Straight lines A and B are plots of expressions (9) and (10) respectively.

by these three Cl^- ions. In NH_4ZnF_3 and NH_4MgF_3 such an effect might be caused by repulsive short-range forces acting between F^- and H^+ which could also flatten the bottom of the well. However, the smaller tunnel frequencies observed in the perovskites than in the hexachlorides indicate that the flattening of the well is not associated with a reduction in the hindering barrier width. In NH_4CdF_3, E_1 is higher than the predictions (9) or (10) and the value of table 1 probably overestimates E_1, but if confirmed, would mean a narrower bottom of the well than in compounds with a similar activation energy. In this case the short-range force should be attractive.

5. Discussion

The height of the barrier which hinders the rotational motion is understood as the minimum energy transfer for the rotor to jump classically from a well to another one, passing above a saddle-point. In the simplest interpretation this 'activation energy' E_a will be the energy of the saddle-point minus the zero-point energy E_0. Svare *et al* (1979) improved the interpretation of the measured E_a for NH_4Cl and NH_4Br considering a zero-point energy correction at the saddle-point due to the transverse degrees of freedom. This last term is usually computed by harmonic approximations or estimated as $\frac{2}{3}E_0$. This gives an overestimation of the barrier, because the rotational potential at the saddle-point is probably flatter than the potential at the bottom of the well. In addition, the fast tunnelling of states slightly below the saddle-point energy would lower the measured E_a.

Under the BNB electrostatic point-charge model the rotational function potential in

the cubic phase was calculated for all members of the series and expressed in terms of the parameters β, $\beta_j (j = 4, 6)$ (Bartolomé *et al* 1977):

$$V_C(\omega) = B\beta[\beta_4 V_4(\omega) + \beta_6 V_6(\omega)] \tag{11}$$

where $B = \hbar^2/2I$, ω represents the set of three Euler angles of one NH_4^+ ion with respect to the lattice frame, and V_j are cubic rotor functions. Since the condition $\Sigma\beta_j^2 = 1$ is imposed, and $\beta_6 > \beta_4$ in all compounds, the barrier height, saddle-points and thus E_0, E_1 and E_a are governed essentially by the non-dimensional parameter β, which ranges between $\beta = 45.5$ for the Mg compound and 25.5 for the Cd one (Palacios *et al* 1986). These compounds correspond to the smallest and largest unit cells respectively. Very recently these calculations have been improved (Smith 1987) by introducing atom–atom potentials of the form

$$\Phi_{HX} = A_{HX} \exp(-\alpha_{HX} r_{ik}) - C_{HX}/r_{ik}^6 - D_{HX}/r_{ik}^8 - q_H q_X / r_{ik}. \tag{12}$$

The first term is the repulsive potential and the r^{-6} and r^{-8} are the first terms of the van der Waals forces. The last one is, of course, the electrostatic term. With a fixed set of potential parameters (table I of Smith 1987) the corrected β and β_j were calculated. The relative weights of the two terms vary a little but do not modify the geometry of the minimum and saddle-points predicted with our previous results. The scaling parameter reduces from $\beta = 45.5$ to 40.2 in the Mg compound and from $\beta = 32.5$ to 20.6 in the Mn compound. Thus, even with the improved potential it is clear that the predicted trend is of diminishing barriers for increasing cell dimensions.

Consequently, the electrostatic model, or the more elaborate one, do not explain the experimental results of the present paper. To be rigorous, our best results of E_a belong to the distorted phase and it has not been properly calculated yet since the atomic positions have not so far been determined. However, the absolute barrier heights are not expected to change drastically above and below T_c, as seen in NH_4ZnF_3 or NH_4MgF_3, and in any case they also follow the same trend.

Since both authors could fit the then available data of NH_4ZnF_3 with $\beta \sim 30$–40 ($E_a = 825$ K), and this parameter depends almost linearly on the activation energy for high barriers, by scaling one gets from $E_a = 1950$ K a value of $\beta \sim 100$ for NH_4CdF_3, very different from $\beta = 25.5$ expected from the theoretical BNB calculations.

The electrostatic model was originally proposed under the assumption that the ammonium perovskites are highly ionic crystals and, therefore, the model proposed for NH_4Cl (Hüller and Kane 1974) was extended. However, other series of compounds could not be explained with such a simple model. In particular, the family of compounds $(NH_4)_2MCl_6$ (M^{4+} = Sn, Pd, Pb, Pt, Ir, . . .) (Svare *et al* 1985), whose structure is Fm3m (FCC) and site symmetry of the NH_4^+ is T_d, has been extensively studied. As in perovskites, the MCl_6 groups form rather rigid octahedra and the NH_4^+ rotates in the space left by four of these groups. As the structure is mainly governed by the ionic radii of M^{4+} and Cl^-, and since the nearest neighbours of an NH_4^+ are always Cl^-, it is possible to study the rotational dynamics on variable inter-ionic distances by varying the tetravalent ion M.

The point-charge model should be applicable in this case since Cl^- is less electronegative than F^-, and forms weaker hydrogen bonds. However the inadequacy of this model was demonstrated (Prager *et al* 1977) when trying to explain the inelastic neutron scattering data of torsional excited states and tunnelling of $(NH_4)_2SnCl_6$. Later the need for repulsive forces was introduced (Otnes and Svare 1979), and more recently (Müller and Hüller 1982) the shape of the rotational potential has been obtained with a pocket-

states formalism from experimental tunnelling frequencies and libration and activation energies. This potential deviates markedly from previous electrostatic calculations, showing flat minima separated by narrow barriers and indicating the pesence of short-range forces.

It is now relevant to note that in the series of hexachlorides the trend of increasing E_a and E_1 and decreasing ω_t for increasing cell size is fulfilled (Prager *et al* 1983a, b) as in the NH_4^+ fluoroperovskites.

A possible reason for this trend may be inferred from the $(NH_4)_2MCl_6$ series due to the similarities found. For $(NH_4)_2PdCl_6$ the pressure dependence of the ground-state tunnel splittings needed the introduction of an effective inter-molecular potential $V(r) = V_0(r_0/r)^n$ with $n = 11 \pm 2$ (Prager *et al* 1983a). This value is indicative of covalent forces in the orientational potential (n = 12–20) rather than electrostatic ones ($n = 4$). One would expect a similar behaviour in our case; however, the tunnelling frequencies found in the present work indicate that the ground-state tunnel splitting could be measured by inelastic neutron scattering (INS) at present, so other types of experiments have to be performed for this check.

The presence of competing repulsive forces may explain this behaviour. In fact, in the temperature-dependent Raman measurements (Agulló-Rueda *et al* 1988) they were considered as causing the 'volume effect' of increasing N–H stretching frequency for decreasing unit-cell size. A pressure study of this vibrational mode (Palacios *et al* 1987) confirms this result.

In short, in the present paper unambiguous evidence is given for the failure of the electrostatic point-charge model as causing the hindered motion of the NH_4^+ ions in ammonium perovskites. The presence of competitive repulsive forces is argued as causing the observed trend of activation energies.

Acknowledgments

Financial support of CICYT–CSIC Grants 3380/80 and PB85-106 is acknowledged. The Kamerlingh Onnes Laboratorium is thanked for hospitality extended to J Bartolomé and E Palacios.

References

Agulló-Rueda F, Calleja J M and Bartolomé J 1988 *J. Phys. C: Solid State Phys.* **21** 1287–97
Bartolomé J, Burriel R, Palacio F, González D, Navarro R, Rojo J A and de Jongh L J 1983 *Physica* B **115** 190–204
Bartolomé J, Navarro R, González D and de Jongh L J 1977 *Physica* B **92** 23–45
Bartolomé J, Palacio F, Calleja J M, Agulló-Rueda F, Cardona M and Migoni R 1985 *J. Phys. C: Solid State Phys.* **18** 6083–98
Brom H B and Bartolomé J 1981 *Physica* B **111** 183–9
Burriel R, Bartolomé J, Navarro R and González D 1984 *Ferroelectrics* **54** 253–6
Cousseins J C and Piña-Pérez C 1968 *Rev. Chim. Miner.* **5** 147–60
Fruchart D 1988 private communication
Garland C W, Lushington K J and Leung R C 1979 *J. Chem. Phys.* **71** 3165–73
Haupt J 1971 *Z. Naturf.* a **26** 1578–89
Helmholdt R, Wiegers G A and Bartolomé J 1980 *J. Phys. C: Solid State Phys.* **13** 5081–8
Hidaka M, Fujii H and Maeda S 1986 *Phase Transitions* **6** 101
Hüller A and Kane J W 1974 *J. Chem. Phys.* **61** 3599
Knop O, Oxton I A, Westerhaus W J and Falk M 1981 *J. Chem. Soc. Faraday Trans.* II **77** 309–20

Morimoto K 1982 *J. Phys. C: Solid State Phys.* **15** 3789–802
Müller W and Hüller A 1982 *J. Phys. C: Solid State Phys.* **15** 7295–304
Navarro R, Burriel R, Bartolomé J and González D 1986 *J. Chem. Thermodyn.* **18** 1135–46
Navarro R, Palacios E, Bartolomé J, Burriel R and González D 1987 *Springer Proc. Phys.* **17** 33–7
O'Reilly D A and Tsang D E 1967 *Chem. Phys.* **46** 1291
Otnes K and Svare I 1979 *J. Phys. C: Solid State Phys.* **12** 3899–905
Palacios E, Bartolomé J, Agulló-Rueda F, Callega J M, Syassen K and Strössner K 1987 *Springer Proc. Phys.* **17** 38
Palacios E, Bartolomé J, Navarro R, García J, González D and Brom H B 1984 *Ferroelectrics* **55** 287
Palacios E, Navarro R, Burriel R, Bartolomé J and González D 1986 *J. Chem. Thermodyn.* **18** 1089–101
Prager M, Press W, Alefeld B and Hüller A 1977 *J. Chem. Phys.* **67** 5126–32
Prager M, Press W, Heidemann A and Vettier C 1983a *J. Chem. Phys.* **80** 2777–81
Prager M, Raaen A M and Svare I 1983b *J. Phys. C: Solid State Phys.* **16** L181–6
Press W 1982 *Springer Tracts in Modern Physics* vol 92 (Berlin: Springer)
Punkkinen M 1975 *J. Magn. Reson.* **19** 222
Raaen A M, Svare I and Fibich M 1982 *Phys. Scr.* **25** 957–60
Riehl J W, Wang R and Bernard H W 1973 *J. Chem. Phys.* **58** 508–15
Rudorff W, Lincke G and Babel D 1963 *Z. Anorg. Allg. Chem.* **320** 110
Smith D 1987 *J. Chem. Phys.* **86** 4055
Steenbergen Ch, de Graaf L A, Bevaart L, Bartolomé J and de Jongh L J 1979 *J. Chem. Phys.* **70** 1450
Svare I 1977 *J. Phys. C: Solid State Phys.* **10** 4137–47
Svare I, Raaen A M and Fimland B O 1985 *Physica* B **128** 144–60
Svare I, Raaen A M and Thorkildsen G 1978 *J. Phys. C: Solid State Phys.* **11** 4069–76
Svare I, Thorkildsen G and Otnes K 1979 *J. Phys. C: Solid State Phys.* **12** 2177–86
Tornero J, Cano F H, Fayos J and Martinez-Ripoll M 1978 *Ferroelectrics* **19** 123–30
Tornero J and Fayos J 1988 Private communication